Advanced Powder Technology 31 (2020) 1441–1456

Contents lists available at ScienceDirect

Advanced Powder Technology

journal homepage: www.elsevier.com/locate/apt

Original Research Paper

Influence of eutectic mixture as a multi-component system in the improvement of physicomechanical and pharmacokinetic properties of diacerein

Rajeshri D. Patel [a], Mihir K. Raval [a,*], Trupesh M. Pethani [a], Navin R. Sheth [b]

[a] Department of Pharmaceutical Sciences, Saurashtra University, Rajkot 360 005, Gujarat, India
[b] Gujarat Technological University, Ahmedabad 382 424, Gujarat, India

ARTICLE INFO

Article history:
Received 25 September 2019
Received in revised form 15 January 2020
Accepted 17 January 2020
Available online 30 January 2020

Keywords:
Diacerein
Eutectic
Kinetic solubility
Cocrystal
Physico-mechanical
Pharmacokinetic parameters

ABSTRACT

A multi-component system of diacerein (DIA) with 2, 4 – dihydroxybenzoic acid (DHA) as coformer at various molar compositions was formulated to simultaneously improve solubility, compressibility and bioavailability of DIA by applying acetone assistant grinding technique. Various evaluation parameters pertaining to measure physicomechanical properties were conducted. Thermal analysis revealed a 'V'-shaped binary phase diagram along with single melting event as a possibility of eutectic formation between drug and coformer. It was further confirmed PXRD and FT-IR. Equidimensional shape with platy nature of eutectic material was observed in SEM images imparting its better flow and compressibility. Solubility and dissolution study showed 2 and 1.8 folds enhancement respectively compared to pure DIA and control batch. Pharmacokinetic study proved 2.1 times higher bioavailability in case of prepared eutectic compared to DIA along with its stable nature. Hence, the multi-component system can become a potential way for the improvement of material characteristics.

1. Introduction

Drug molecules with limited aqueous solubility and dissolution are becoming common in the research and development portfolios of discovery focused on pharmaceutical industries. It is estimated that more than 70% of potential drug molecules in the development pipeline are poor in their physicochemical properties. Moreover, drug candidates in spite of desired pharmacological activity face numerous difficulties in development and commercialization due to their unfavourable solubility, dissolution rate, mechanical properties, stability, manufacturability and so on [1].

It is not worth for manufacturing of solid orals if only physicochemical properties improvement is focused. If the material improves mechanically also along with physicochemically then and then the purpose of the pharmaceutical industry is served [2,3]. In recent times, manipulating of solid-state properties adopting the principle of crystal engineering approach has extensively been employed in the pharmaceutical research field as a new strategy to diversify notably the multi-component solid forms [4]. They can lead to improving the physical attributes including their solubility, bioavailability, stability toward thermal and humidity stress, flowability, manufacturability and pharmacokinetics parameters without changing the efficacy of the drug [5]. Fig. 1 illustrates the formation of new salt [6], polymorphs [7], solvate [8], hydrate [9], cocrystal [10], eutectic [11], solid solution [12], and co-amorphous system [13]. Among these, salt formation can modify the pharmaceutical properties of ionisable APIs through covalent bonding while remaining multi-component solid forms can effectively improve the aforesaid properties of non-ionisable or poorly ionisable APIs with counter molecule/coformer using non-covalent interaction such as hydrogen bonding, π-π stacking, dipole interaction or Van der Waals forces [14].

The multi-component solid formation is the result of molecular association between similar materials (homomolecular) or distinctive materials (heteromolecular) interactions. In the case of strong adhesive (hetero) interactions between participating molecules predominate the cohesive (homo) interactions of constituent components, and then cocrystals are generated. In contrast, if the cohe-

Abbreviations: DIA, diacerein; DHA, 2,4-dihydroxy benzoic acid; DSC, differential scanning calorimetry; PXRD, powder X-ray diffraction; FT-IR, Fourier transform infrared spectroscopy.

* Corresponding author: Department of Pharmaceutical Sciences, Saurashtra University, Rajkot 360 005, Gujarat, India.
E-mail address: mkraval@sauuni.ac.in (M.K. Raval).

https://doi.org/10.1016/j.apt.2020.01.021

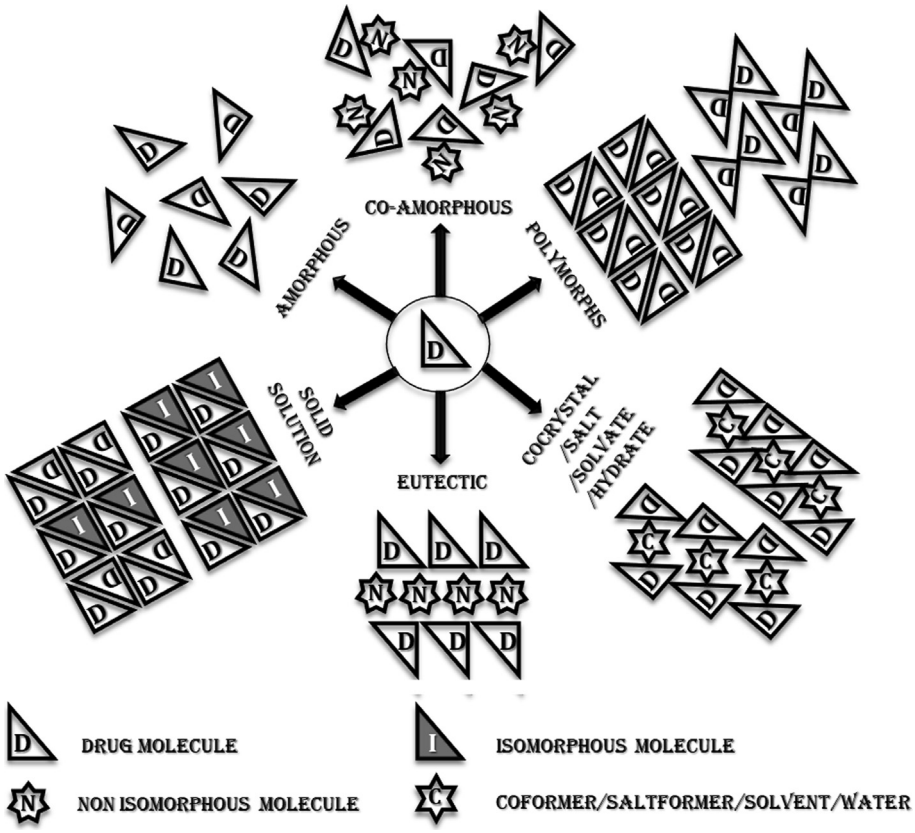

Fig. 1. Schematic illustration of multi-component solid forms.

sive (homo) interactions dominate between isomorphous materials, solid solutions are produced whereas for non-isomorphous materials, resulting eutectics formation as can be defined the multi-component system having a lower melting point than the individual components [15,16].

Eutectic formation of poor functionality API in presence of coformer has been reported for improving biopharmaceutical performance. Sangamwar et al. investigated for the eutectic mixture of α-eprosartan with p-hydroxybenzoic acid in 1:3 stoichiometry ratio which exhibited improved physicochemical and pharmacokinetic behaviour compared to parent drug [17]. Patel et al. explored the formation of a eutectic mixture through the temperature-composition binary diagram to improve the functionality of nimesulide with nicotinamide [11]. Vasisht et al. prepared highly soluble eutectics with enhanced biological efficacy of hesperetin [18]. Dalvi and Sathisaran generated the eutectic system for curcumin-salicylic acid system with better solubility than pure drug [19]. Bansal et al. studied that the microstructure of aspirin-paracetamol eutectic system presented superior compressibility, tabletability and compactibility as compared with the physical mixture of that system [20]. Various other APIs and their eutectics like felodipine-nicotinamide [21], etodolac with paracetamol and propranolol hydrochloride [22], hydrochlorothiazide-atenolol [23] and simvastatin-aspirin [24] have been reported for their improved properties.

Diacerein (DIA, Fig. 2) chemically called 4,5-bis(acetyloxy)-9,10-dihydro-9,10-dioxo-anthracene-2-carboxylic acid, is a chondroprotective agent used for the treatment of osteoarthritis with mild analgesic, antipyretic and anti-inflammatory activity, metabolized to active rhein [25]. DIA belongs to BCS class II drug with poor solubility (3.197 mg/l) which limits its oral bioavailability (35–56%) [26]. DIA is a crystalline yellow powder with pKa of

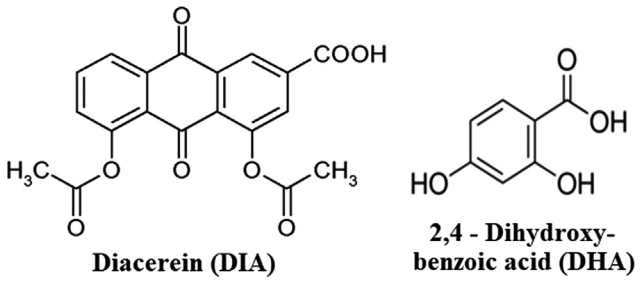

Fig. 2. Chemical structures of Diacerein (DIA) and 2,4 – Dihydroxy benzoic acid (DHA).

3.01, shows pH-dependent solubility. Moreover, DIA exhibits very poor mechanical characteristic in concern with flow properties [27]. Formulation approaches such as self nanoemulsion, solid dispersion, complexation, nanofiber and nanoparticles [28–32] have been attempted to improve the physicochemical and pharmacokinetic properties.

In the majority studies which have been published so far, are lacking in explaining the way how to formulate binary phase diagram using results obtained from differential scanning calorimetry (DSC) study. The present investigation has been performed to explore the applicability of the binary phase diagram, the way of its formation to young researchers. In this work, solvent assistant grinding method has been employed because it imparts high molecular mobility for the reaction between drug and coformer. Apart from being a simple method, detection of the multi-component system can be made using least quantity without any significant wastage [18]. Finally, the prepared material was converted into tablets using direct compression technique.

2. Materials and methods

2.1. Materials

DIA (Pure drug) was procured as a gift sample from Ami Lifesciences Pvt. Ltd. (Baroda, India) with batch no. DSN/40400615. Rhein (Active metabolite of DIA) was purchased from Yucca Enterprises (Wadala, Mumbai). 2,4-Dihydroxybenzoic acid (DHA) as coformer was procured from Sisco Research Laboratories Pvt. Ltd. (Mumbai, India) and used as received. Lactose monohydrate and Microcrystalline cellulose 102 (MCC) were procured from Sisco Research Laboratories Pvt. Ltd. (Mumbai, India) and Yarrow Chem Products (Mumbai, India). All other chemicals and solvents used were of chromatographical or analytical grade. Distilled water was generated from a Millipore Direct-Q water purification system (Merck Millipore Pvt. Ltd., India).

2.2. Preparation and prediction of multi-component solid form by constructing DIA-DHA phase diagram

Binary mixtures of DIA/DHA in % molar compositions of 100/0, 90/10, 80/20, 70/30, 60/40, 50/50, 40/60, 30/70, 20/80, 10/90, 0/100 combined (Approx 200 mg batch scale) were subjected to manual grinding for 30 min using an agate mortar pestle by adding few drops ($\approx$ 200 μl) of acetone to aid mixing between components. The obtained mass was scratched out, dried in an oven (40 °C) for 2 h followed by gentle trituration before sieving through a 100 mesh (ASTM standard) before further analysis. The resulting products were subjected to DSC for ascertaining the formation of multi-component solid forms. A phase diagram was constructed by taking solidus and liquidus temperatures of various grounded mixtures [33]. The remaining products were stored in the glass vials inside a desiccator. The same procedure was followed for drug alone by omitting the coformer DHA (Control batch). DIA-DHA physical mixture was prepared by gently blending of both the components in the optimized molar composition in agar mortar pestle without use of acetone immediately before the use.

2.3. Solid-State characterization

2.3.1. Thermal analysis

Thermal analysis of the grounded samples was performed with help of DSC (DSC 60, Shimadzu, Japan) previously calibrated for temperature and heat flow accurately using indium metal standard. Accurately weighed samples (2–3 mg) were placed in hermetically sealed aluminium pans and analyzed from 40 to 300 °C at a scan speed of 5 °C/min using a sealed aluminium empty crucible as reference. An inert atmosphere was maintained by purging nitrogen gas at a flow rate of 100 ml/min.

2.3.2. Powder X-ray diffraction analysis (PXRD)

The PXRD patterns of pure drug, control batch and prepared samples were collected on PANalytical diffractometer system (X'Pert pro Multi-Purpose Diffractometer, Philips, India) with Cu-Kα X-radiation at voltage 40 kV and current 30 mA. X'Pert HighScore Plus software was used to collect and plot the diffraction patterns. The instrument was operated over 2θ scale with an angular range of 10–40° at a scan rate of 0.0499°/s.

2.3.3. Fourier transform infrared (FT-IR) spectroscopy

FT-IR spectroscopy (Cary-630, Agilent Technologies, USA) was used for recording the IR spectra of the samples. The spectra were recorded using the ATR technique (Diamond ATR crystal, Agilent Technologies, USA) and collected by the Lab solution software. All the spectra were acquired in the region of 400–4000 cm^{-1} with 4 accumulative scans having a resolution of 4 cm^{-1}.

2.3.4. Scanning electron microscopy (SEM)

The shape and surface morphology of the samples was analyzed using SEM (JSM-6380, Jeol, Japan) operating at 10 kV with an image analyzer. The powder samples were dispersed on an aluminium stub with double-faced adhesive tape. The mounted samples were prepared electrically conductive by coating the powder with a thin layer of gold by using the sputter coater instrument. The prepared stubs were placed in the microscope and the images were observed and recorded at the magnification range of 2500× to 10,000×.

2.3.5. Hot stage microscopy (HSM)

The HSM was done on Linkam Scientific Instruments Ltd provided hot stage and TMS 94 temperature controller, fitted on an optical Microscope (NIKON) with Q imaging camera to capture the images. The sample was focused under the microscope at 10X zoom with the images collected every second during the heating process wherein the samples are heated from 50 °C to 100 °C at 10 °C/min, followed by heating to 250 °C at 5 °C/min, and finally to 300 °C at 10 °C/min.

2.4. Physicochemical and mechanical parameters

2.4.1. Flow characterization

The flowability of the powder was determined by measuring Angle of repose, Carr's Index (CI) and Hausner's ratio. The angle of repose was estimated by fixed funnel method using Eq. (1). CI and Hausner's ratio were calculated from bulk and tapped densities of the powder. Tapped densities of the samples (20 gm) were measured in a 100 ml measuring cylinder using a tapped density machine (ETD-1020, Electrolab, Mumbai, India) [34].

$$\theta = tan^{-1}\frac{h}{r} \tag{1}$$

where θ = angle of repose; h = height of the pile; r = radius of the base pile

$$Carr'sindex = \lfloor\frac{tapped\ \ density - bulk\ \ density}{tapped\ \ density}\rfloor \times 100 \tag{2}$$

$$Hausnarratio = \lfloor\frac{tapped\ \ density}{bulk\ \ density}\rfloor \tag{3}$$

2.4.2. Analysis of packability, compressibility and compactibility

2.4.2.1. Packability study. To minimize the effect of different particle size among pure drug, control batch and prepared samples, all the samples were sieved through a 100-mesh sieve. Packability study was explored by Kawakita analysis using a tap density tester USP (Electrolab, ETD-1020, India). Briefly, bulk and tapped densities of powder samples were estimated by calculating the change in volume of powder level into a 100 ml measuring cylinder was recorded after 100, 300, 500, 750, 1200 to 2000 taps in tap density tester.

For Kawakita equation

$$\frac{n}{c} = \frac{n}{a} + \frac{1}{ab} \tag{4}$$

where, n = tap number; C = volume reduction; C can be calculated according to the following equation.

$$C = \frac{V_0 - V_n}{V_0} \tag{5}$$

where V_0 and V_n are the powder bed volumes at initial and n^{th} tapped state, respectively. *a* and *b* are the Kawakita constants; *'a'* defines as initial porosity of the powder which explains the total degree of volume reduction for the bed of particles at infinite applied pressure and *'1/b'* expresses pressure needed to compress the powder to one half of the total volume.

The values of *'a'* and *'b'* were calculated from the slope and intercept of the kawakita plot of $\frac{n}{c}$ Vs *n*, respectively [35]. The data produced in Kawakita plot was analysed using Kuno's equation:

$$ln(q_t - q_n) = -Kn + ln\,(q_t - q_0) \quad (6)$$

where, q_0, q_n and q_t are the initial density, density at 'n^{th}' taps and density at infinite taps, respectively; *Kn* is the Kuno's constant represents the rate of packing process. *a*, *b* and *Kn* are the constants assess the packability of powder was assessed by comparing the constants. Rearrangement index (ab index) expresses the evaluation of particle rearrangement during compression which is derived from the Kawakita constant *'a'* and *'b'*. The ab index was calculated as the reciprocal of the intercept of the extrapolated part of the Kawakita plots [36].

2.4.2.2. Heckel study. Compactibility and compressibility were addressed by measuring tensile strength and Heckel analysis of the compact. The compacts of pure drug, control batch and eutectic sample were prepared by accurately weighing 200 ± 5 mg of each sample and manually filled into 10-mm flat-faced punch in KBr press (Techno-search Instruments, Mumbai, India). During the experiment, it was found that the compacts were laminated immediately upon ejection from die. This problem was solved by adding a small amount of 2% w/w MCC as a directly compressible excipient to each sample. The samples were compressed under different compression force ranging from 1 to 9 tons (9.8×10^3 to 88.26×10^3 Newton) by keeping 1 min dwell time. The punch and die were lubricated using 1% w/v dispersion of magnesium stearate in acetone before compaction process [37]. True density was considered as mass per volume of the compact at a maximum applied force in tons [38] (Here, 9 tons). Eq. (7) represents the compression behaviour of prepared samples as parameters of Heckel equation.

$$ln\left[\frac{1}{(1-D)}\right] = KP + A \quad (7)$$

where D (=ρ_A/ρ_T) is the relative density of compacts at applied pressure P; ρ_A and ρ_T are the density at pressure P and true density, respectively; ε (=1-D) is the porosity of powder; K is the slope and A (Y-intercept) are regression coefficients of linear plot of ln [1/ (1-D)] Vs P curve i.e. heckle plot. Reciprocal of K denotes mean yield pressure (Py) and A expresses the densification of powder bed at low pressure. Yield strength (σ0) represents the material ability to undergo deformation or fragmentation. It can be calculated by 1/3 K.

2.4.2.3. Tensile strength and elastic recovery measurement. The compacts prepared from Heckel analysis were subjected to the tensile strength measurement. The diameter (D) and thickness (T) were measured using a digital vernier caliper (Mitutoyo, Japan) after 24 h, and a crushing strength (P) was measured with the help of a digital hardness tester (Electrolab Pvt. Ltd., India). The tensile strength (T, Kg) of the compacts was calculated using Eq. (8) [39].

$$T = \frac{0.0624 \times P}{D \times T} \quad (8)$$

The elastic recovery was performed for determining the retained energy during the compression process and released after the compression process. The elastic recovery can be calculated using the thickness before (Hc) and after (He) being stored for 24 h using Eq. (9) [40].

$$\%\ ER = [(He - Hc)\ /Hc]\ X\ 100 \quad (9)$$

2.4.3. Formulation and evaluation of directly compressible tablets

Tablets of pure drug, control batch and prepared samples were formulated using direct compression technique. The manufacturing formulas and post evaluation parameters of the prepared tablets are given in Table 1. The specific amounts of sieved pure drug, control batch and prepared samples were mixed separately with sufficient portions of excipients to formulate around 40 tablets from each batch. The individual blends were introduced manually into the die and compressed by 12 mm round and concave faced punch using eight-station rotary tablet machine (Karnawati engineering Ltd., India). The tablets were ejected and stored in screw-capped bottles for 24 h before using, to allow for possible hardening and elastic recovery. The tablets were also taken for in-process and finished product evaluation tests. Weight variation test was carried out by weighing 20 tablets individually and then calculating the average weight. The thickness of the tablets was obtained by digital vernier caliper (Mitutoyo, Japan). Hardness and friability of tablets were measured with the help of digital hardness tester (Electrolab Pvt. Ltd., India) and Roche friabilitor (EF-2, Electrolab Pvt. Ltd., India), respectively. Disintegration test was performed for six tablets using disintegration test apparatus (ED2, Electrolab Pvt. Ltd., India) at 37 ± 1 °C in 900 ml of distilled water according to the Indian Pharmacopoeia 2010 [40].

2.4.4. High performance liquid chromatography (HPLC) method development

Quantification of drug in prepared sample was analyzed using the HPLC system (Shimadzu Corporation, Japan) which consisted of a CTO-20AC thermostated column oven and SIL20AC autosampler, and coupled with a SPD-M 20A PDA detector. Data acquisition and processing were performed using Lab solution software (version 5.53 SP3C) from Shimadzu Corporation, Japan. Chromatographic separations were achieved on a Phenomenex Gemini C18 column (250 mm × 4.6 mm, 5 μ pore size) placed in thermostated column oven at 40 °C. The mobile phase, comprising of acetonitrile (ACN; A) and ammonium acetate buffer (10 mM; pH 3; B), was eluted through the gradient system as follows: 80% → 30% B at 0.0–8.0 min; 30% → 60% B at 8.0–12.0 min; 60% → 80% B at 12.0–14.0 min. The flow rate and sample injection volume were

Table 1
Manufacturing formulas and post compression evaluation parameters for the preparation of directly compressible tablets.

Ingredients	Amount per tablet (mg)		
	Pure drug	Control batch	DIA-DHA prepared sample
Diacerein IP	50	50	112.8 (equivalent to 50 mg DIA)
Lactose monohydrate	115	115	77.2
Microcrystalline cellulose (Avicel PH-102)	25	25	5
Aerosil-200	25	25	20
Sodium starch glycolate	25	25	25
Magnesium stearate	5	5	5
Talc	5	5	5
Total weight of tablet	**250**	**250**	**250**
Weight variation (mg)*	250.2 ± 2.43	249.4 ± 3.12	248.7 ± 2.58
Thickness (mm)*	3.39 ± 0.07	3.34 ± 0.08	3.44 ± 0.15
Hardness (kg/cm^2)*	4.9 ± 0.31	5.1 ± 0.25	5.6 ± 0.36
Friability (% loss)*	0.36 ± 0.08	0.35 ± 0.07	0.30 ± 0.06
D.T.(sec)*	65.33 ± 2.52	58.00 ± 2.65	47.33 ± 2.08

* Indicates data shown as mean ± SD (n = 3).

set at 0.8 ml/min and 5 μl, respectively. Analytical run time was 14 min and absorbance was detected at 254 nm.

2.4.5. % Yield and drug content

The % yield of the prepared sample was determined using Eq. (10). Drug content of DIA in the produced sample was estimated by dissolving 10 mg of prepared sample in 1 ml of DMSO and further diluted up to 10 ml with ACN. After appropriate dilution, the samples were analyzed using HPLC method as described above. Content determination of drug was performed in triplicate and the average and standard deviation were calculated.

$$\%\text{Yield} = \frac{\text{Total weight of prepared sample}}{\text{Total weight of drug and coformer}} \times 100 \quad (10)$$

2.4.6. Kinetic solubility measurement

Kinetic solubility of pure DIA and DIA-DHA samples was estimated in different buffer solutions in triplicate, namely pH 1.2 (Hydrochloric acid buffer), pH 4.5 (Acetate buffer), and pH 6.8 (Phosphate buffer) as buffers were prepared using the standard pharmacopoeial method as recommended by IP. An equivalent amount of powder materials corresponding to 50 mg of DIA were dispersed to a flask containing 200 ml mentioned buffers separately. The resultant suspension was kept in a shaker-incubator equipped with a temperature controlling system (Tempo Instruments and Equipments Pvt. Ltd., India) at 37 ± 0.5 °C with an agitation speed of 150 rpm for 24 h to allow saturation. The samples (5 ml) were withdrawn at the predefined time intervals (5, 10, 15, 30, 45, 60, 120, 180, 240, and 1440 min), and the equal volume of aforementioned buffers was supplemented. The resulting samples were filtered through a 0.45 μm PVDF syringe filter (Millex-HV, Millipore) and the filtrate was suitably diluted and analyzed by HPLC method for the quantification of the drug in all samples as mentioned in Section 2.4.4.

2.4.7. In-vitro drug release profile

Powder dissolution measurements of DIA, control batch, DIA-DHA physical mixture and prepared samples were performed using dissolution apparatus USP type-I (Electrolab TDT-06P, USA). First, the starting powder materials were sieved through 100-mesh sieves (ASTM) to ensure the particle size less than 150 μm. Each sample, equivalent to 50 mg DIA was filled in hard gelatine capsule (size 0) in triplicate and placed in dissolution vessels containing 900 ml different dissolution media, namely distilled water, pH 1.2 (Hydrochloric acid buffer), pH 4.5 (Acetate buffer), and pH 6 (Citrate buffer) at 100 rpm maintained at 37 ± 0.5 °C. Whereas, tablet dissolution profiles of DIA, control batch and prepared samples were performed using dissolution apparatus USP type-II (Electrolab TDT-06P, USA). The tablets were placed in dissolution vessels containing 900 ml of citrate buffer (pH 6) at 75 rpm maintained at 37 ± 0.5 °C [41]. 5 ml of aliquot was withdrawn from dissolution basket at the specific time intervals up to 2 h and replaced with fresh above mentioned dissolution media to maintain sink condition. The samples were filtered immediately and subjected to HPLC analysis as mentioned in Section 2.4.4. The independent model was applied to evaluate the dissolution profiles of powder and tablet on basis of their dissolution percent (% DP), dissolution efficiency (% DE), difference factor f_1, similarity factor f_2 and MDT *in vitro* [42].

The difference factor f_1 and similarity factor f_2 were measured to evaluate in the percentage dissolution between two dissolution curves as expressed in Eqs. (11) and (12).

$$f_1 = \left[\left(\sum_{t=1}^{n}(R_t - T_t)\right) / \left(\sum_{t=1}^{n} R_t\right)\right] \times 100 \quad (11)$$

$$f_2 = 50 \times \log\left[\left(1 + \left(\frac{1}{n}\right)\sum_{t=1}^{n} w_t(R_t - T_t)^2\right)^{-0.5} \times 100\right] \quad (12)$$

where R_t is the percentage dissolved of reference at the time point t; T is the percentage dissolved of test at the time point t; n is the number of withdrawal points. For the dissolution profiles to be considered similar, f_1 values should be close to 0, and f_2 values should be close to 100. Generally, f_1 values up to 15 (0–15) and f_2 values greater than 50 (50–100) indicates that the dissolution profiles are similar whereas smaller value expresses an increment in dissimilarity between release profiles.

2.5. Pharmacokinetic study

2.5.1. Animals

Sprague-Dawley rats weighing 200–250 g, were housed in polypropylene cages under the standard conditions of temperature (25 ± 1 °C), relative humidity (55 ± 10%) cycle and standard food and filtered water were supplied *ad libitum*. The animals were kept 12 hrs light/dark cycles for acclimatization for one week and fasted overnight with free access to water prior the experiment. The animal protocol was approved by the Institutional Animal Ethics Committee (IAEC), constituted as per guidelines of the Committee for Purpose of Control and Supervision of Experiments on Animals Government of India (IAEC/DPS/SU/1609; dated 12th December 2016).

2.5.2. Experimental protocol

Twenty four Sprague-Dawley rats were randomly distributed in two groups (n = 12). Group I and II were administered with pure DIA and prepared samples orally in water containing 0.2% w/v sodium carboxymethyl cellulose as a suspending agent at a dose equivalent to 30 mg/kg body weight of DIA, respectively. Serial blood samples were collected from the retro-orbital plexus of the rats at 0 (predose), 0.25, 0.5, 0.75, 1, 1.5, 2, 4, 6, 12, and 24 h plastic tubes containing heparinized saline as an anticoagulant. Plasma samples were harvested by centrifuging (Centrifuge 5418R, Eppendorf AG, Germany) the blood at 10,000 rpm for 20 min at 4 °C and stored at −20 °C before analysis. A simple protein precipitation method was employed for the extraction of drug from the rat plasma and quantified using HPLC analysis. Briefly, 500 μl of each plasma sample was mixed with 50 ml internal standard (IS), p-Aminobenzoic acid (100 μg/ml) and vortexed for 60 sec. A 500 μl volume of ACN as extraction solvent was added and vortexed for 10 min. The resulting mixture was centrifuged at 10,000 rpm for 10 min at 4 °C. The supernatant (500 μl) was collected and dried it at 60 °C for 2 h. The dried residues were reconstituted with mobile phase (100 μl) and vortexed it for 5 min prior to the injection in the HPLC system.

2.5.3. HPLC analysis for quantification of drug in rat plasma

When DIA enters into the blood circulation, it converts into its active metabolic form *rhein*. Hence, the HPLC method was developed for the detection of rhein in blood plasma of rat [25]. The procedure followed as described in Section 2.4.4 with slight modification. The mobile phase, comprising of ACN (A) and ammonium acetate buffer (10 mM; pH 3; B), was eluted through the gradient system as follows: 80% → 30% B at 0.0–8.0 min; 30% → 60% B at 8.0–10.0 min; 60% → 80% B at 10.0–18.0 min. The analytical run time and sample injection volume were modified to 18 min and 20 μl, respectively. The concentration range of the standard curve was kept 0.2 to 20 μg/ml of rhein with correlation coefficient (r^2), 0.999.

Table 2
Theoretical prediction of multi-component adduct using ΔpKa rule.[43]

No.	Drug/Coformers	pKa (acidic)	pka (basic)	ΔpKa When DIA as a acid	Inferance
1	Diacerein	3.01	–	–	–
2	Nicotinamide	13.39	3.63	0.62	may form cocrystal/ salt
3	4-Aminobenzoic acid	2.38	4.85	1.84	may form cocrystal/ salt
4	Glutaric acid	3.76	4.34	1.33	may form cocrystal/ salt
5	Nicotinic acid	2.2	4.8	1.79	may form cocrystal/ salt
6	Oxalic acid	1.25	4.14	1.13	may form cocrystal/ salt
7	2,4-Dihydroxybenzoic acid	3.33	−5.8	−8.81	may form cocrystal
8	Salicylic acid	3.01	−6.3	−9.31	may form cocrystal
9	Succinic acid	3.55	4.25	1.24	may form cocrystal/ salt
10	Urea	15.73	−2.4	−5.41	may form cocrystal
11	L-Aspargine	2.02	8.8	−0.99	may form cocrystal
12	Aspartic acid	2.09	9.82	−0.92	may form cocrystal
13	Acetamide	16.75	−1.3	−4.31	may form cocrystal
14	p-Aminosalicylic acid	3.58	2.21	−0.8	may form cocrystal
15	Aceclofenac	3.44	−2.1	−5.11	may form cocrystal

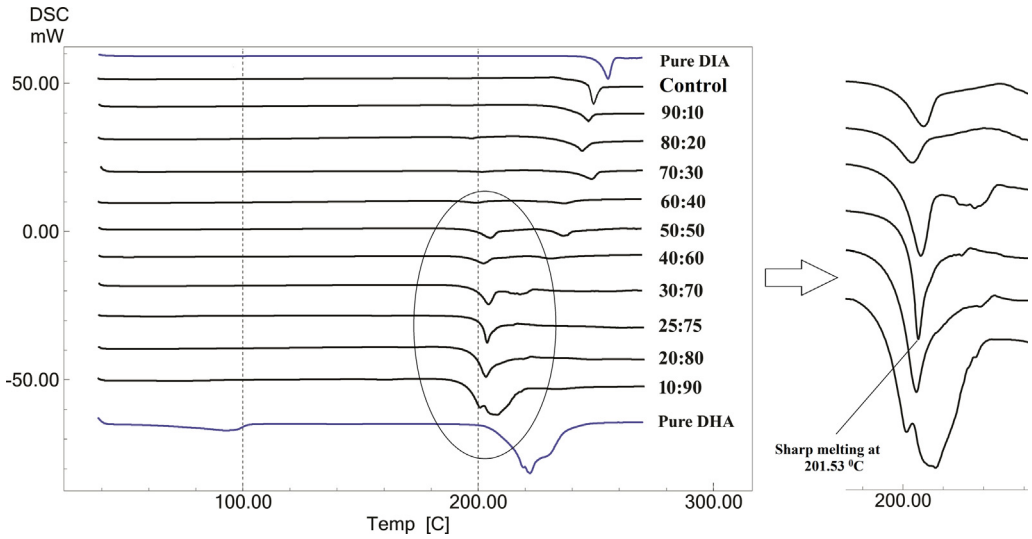

Fig. 3. Overlay of DSC scan for screening the multi-component solid form of different molar compositions of DIA and DHA.

Table 3
Temperatures of solidus, liquidus, melting points of components and ΔH_{fus} for binary phase diagram system.

DIA:DHA	$T_{solidus}$/°C	$T_{liquidus}$/°C	T_m (DHA)/°C	ΔH_{fus} (J/g) (DHA)	T_m (DIA)/°C	ΔH_{fus} (J/g) (DIA)
100:00	–	–	–	–	255.17	96.68
Control	–	–	–	–	249.02	151.96
90:10	191.65	249.10	195.89	1.73	246.84	44.33
80:20	192.73	248.24	197.25	6.03	244.21	80.45
70:30	196.90	251.32	201.60	6.26	248.27	64.45
60:40	193.31	242.84	199.14	8.64	236.34	38.54
50:50	198.54	240.62	205.20	75.37	236.03	51.69
40:60	195.68	246.01	202.25	60.69	231.48	20.99
30:70	199.13	222.88	204.39	82.94	217.87	27.62
25:75	201.53	206.94	–	–	–	364.67
20:80	198.38	208.30	–	–	–	254.52
10:90	195.87	216.66	208.04	474.79	233.17	4.22
00.100	–	–	222.05	598.80	–	–

Temperature of solidus; $T_{solidus}$, temperature of liquidus; $T_{liquidus}$, melting temperature; T_m and heat of fusion; ΔH_{fus} obtained from DSC heating runs of mixtures of DIA and DHA.

2.6. Stability study

Prepared DIA-DHA samples (powder and tablet formulation) were assessed to accelerated stability study as per International Council for Harmonisation (ICH) guideline for six months. Samples were put in screw-capped glass bottles separately at 40 °C/75% RH in the stability chamber (SC-16 PLUS, Remi, India). At the end of the study, samples were evaluated by comparisons of dissolution profiles and characterized by DSC, FT-IR and PXRD analysis.

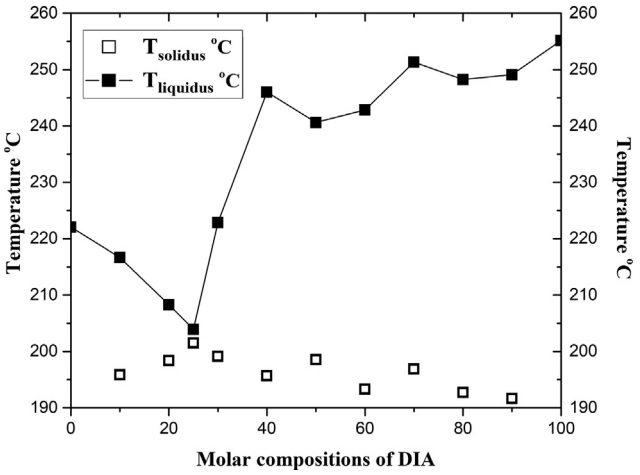

Fig. 4. Binary phase diagram of DIA-DHA system (The temperatures of solidus are shown in open square and the temperatures of liquidus are shown in close square).

3. Results and discussion

DIA is a weakly acidic drug with pKa of 3.01 and has functional groups (Fig. 2) which are found to have propensities to generate multi-component adducts through hydrogen bond interaction. A very simple ΔpKa rule (ΔpKa = pKa of conjugated acid of the base (coformer) - pKa of acid (DIA)) was applied to predict the appropriate coformers that may form a cocrystal or a salt. If the ΔpKa < 0 may result in a cocrystal, ΔpKa > 3 often gives a salt and ΔpKa between 0 and 3 may form either a cocrystal or a salt [43]. The pka and ΔpKa values of the selected coformers for the theoretical prediction of multi-component adduct using ΔpKa rule as listed in Table 2.

In this context, SAG method with its advantages of reduced time and efficient atomic reaction over neat grinding was applied as a preliminary screening method to identify any interaction between drug and coformer and also to determine their stoichiometry [44]. Here, a solid form screening was investigated in a 1:1 and occasionally 1:2 stoichiometric ratio of drug with fourteen coformers. Each sample was prepared by addition of

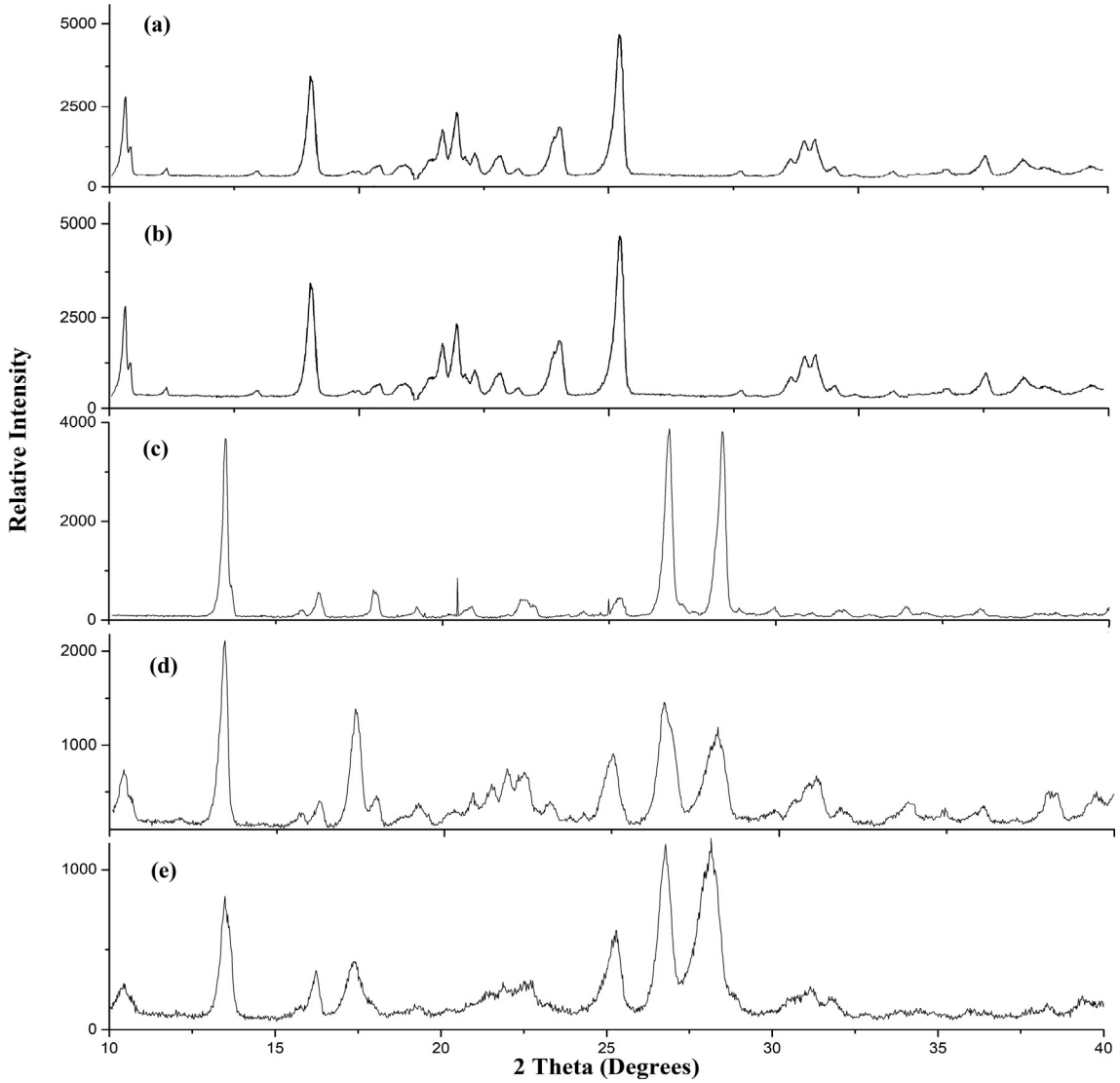

Fig. 5. PXRD patterns of DIA (a); Control batch (b); DHA (c); DIA-DHA physical mixture (d) and DIA-DHA eutectic (e).

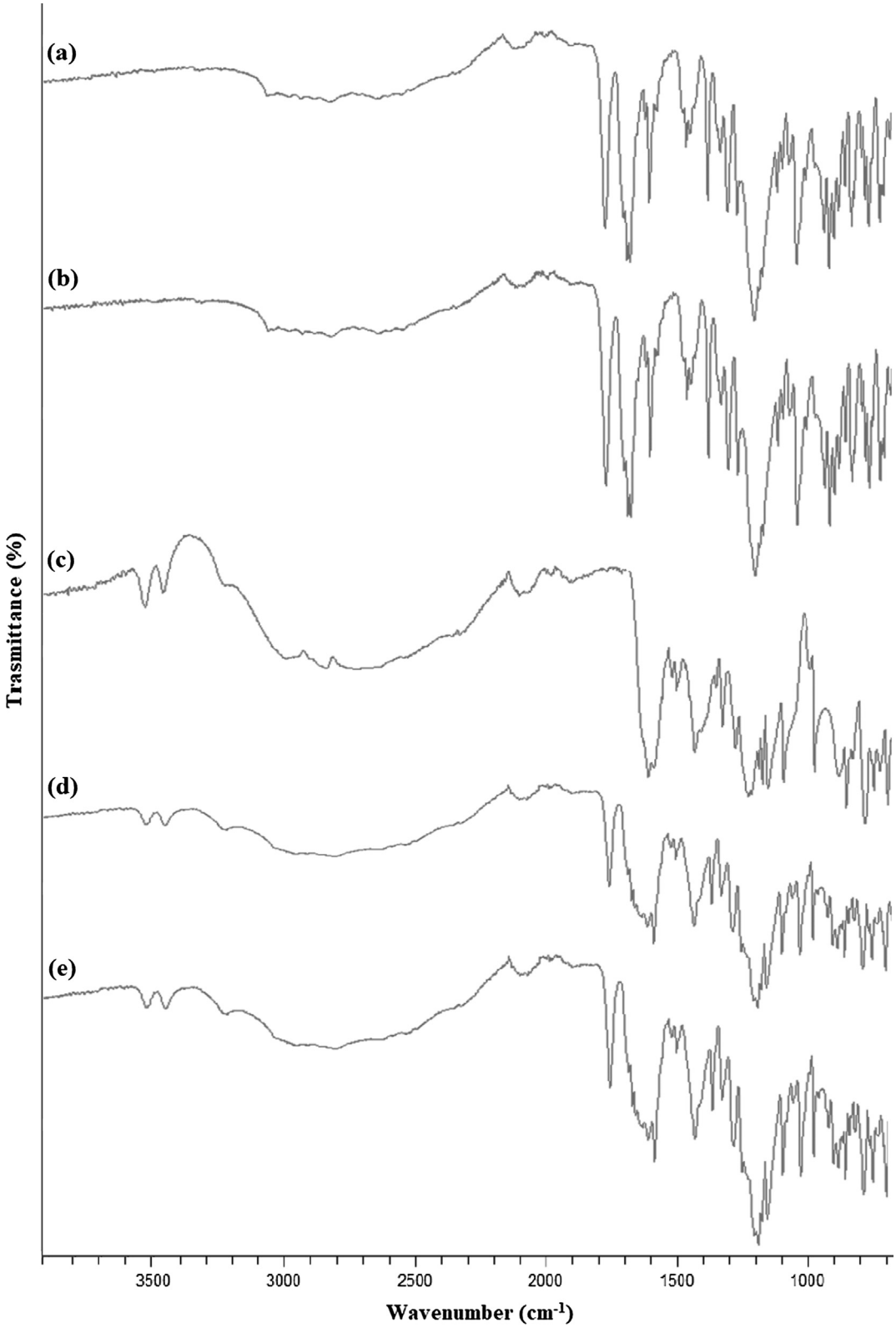

Fig. 6. ATR-FTIR spectra of DIA (a); Control batch (b); DHA (c); DIA-DHA physical mixture (d) and DIA-DHA eutectic (e).

few drops of different polarity organic solvents such as acetone, methanol, ethanol, and ACN into the physical mixture of drug and coformer in the various molar ratios followed by trituration for 30 min (Table SI1 given in supplementary information). The solvent selection was made based on at least the partial solubility of drug and coformer in that particular solvent. The partial solubility of both components was required to initiate the interaction between each other.

3.1. Solid-state characterization

3.1.1. Thermal analysis

DSC thermograph of DIA and control batch depicted a sharp endothermic melting point at 255.17 °C (ΔH_{fus} = 96.68 J/g) and 249.02 °C (ΔH_{fus} = 151.96 J/g), respectively which indicated their crystalline nature [32]. Control batch showed slight depression in melting peak due to trituration in presence of solvent [45]. DHA showed a broad endothermic region nearly 213 to 228 °C with a melting peak at 222.05 °C (ΔH_{fus} = 598.80 J/g). The DSC overlay of pure DIA, control batch, pure DHA and DIA-DHA binary mixtures are represented in Fig. 3. It was observed that from the molar compositions 90:10 to 10:90, the melting point of drug and coformer showed significant depression which is mentioned in Table 3. DSC thermograms of 30:70 and 20:80 M compositions revealed the peak positions of drug and coformer in very close proximity. It might be a sign of positive interaction between the components towards the formation of eutectic or cocrystal. Looking at such peak position, a molar composition of 25:75 (the intermediate composition of DIA: DHA) was prepared and studied for its thermal behaviour. A single sharp endothermic melting peak appeared at 201.53 °C (ΔH_f = 364.67 J/g) which was a sign of positive interaction between both the components. A phase diagram was constructed by drawing solidus and liquidus temperatures of pure components and various molar compositions (Fig. 4). All the points showing liquidus temperature were connected to draw the phase

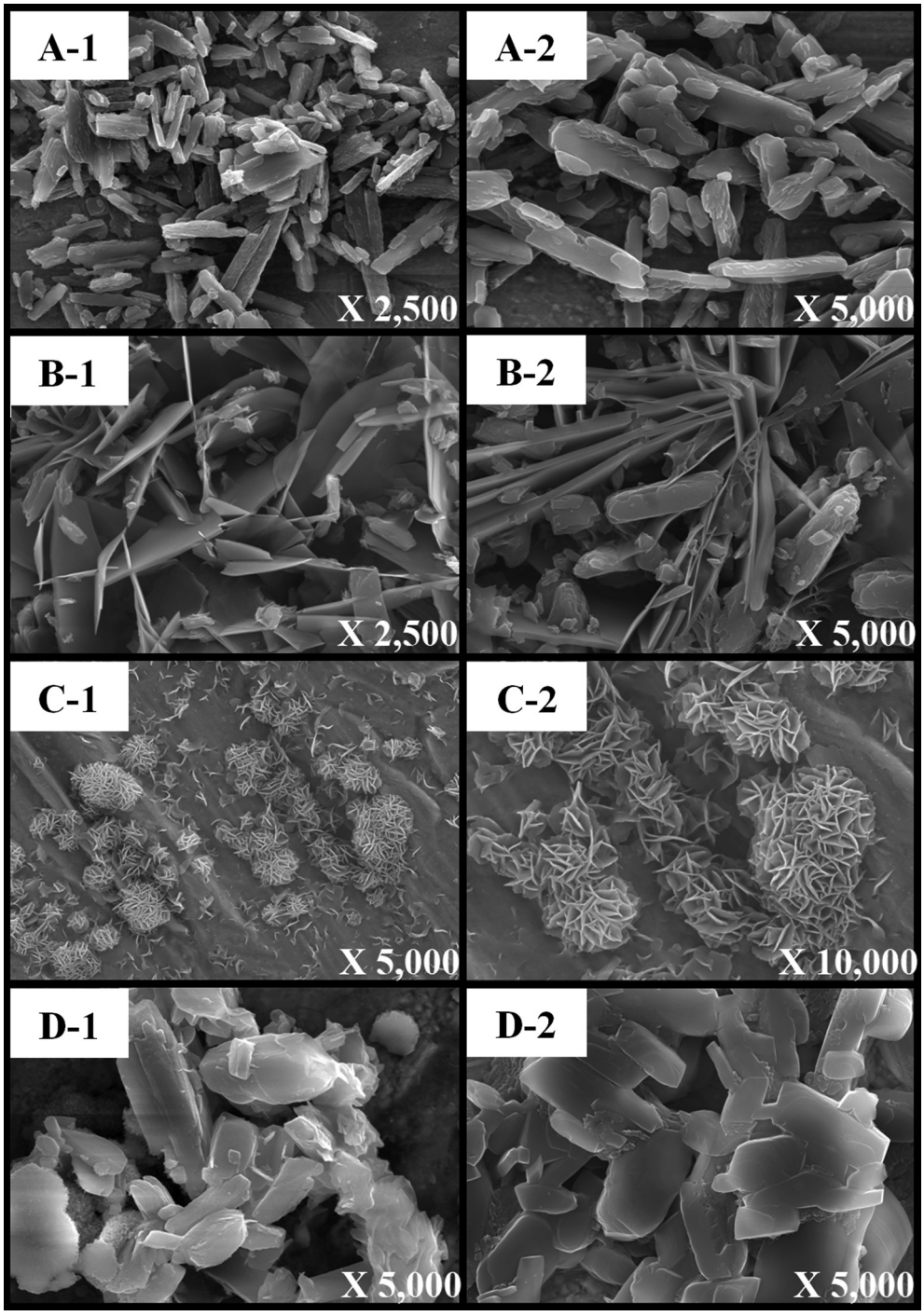

Fig. 7. Scanning electron micrographs of DIA (A-1 & A-2); Control batch (B-1 & B-2); DHA (C-1 & C-2) and DIA-DHA eutectic (D-1 & D-2).

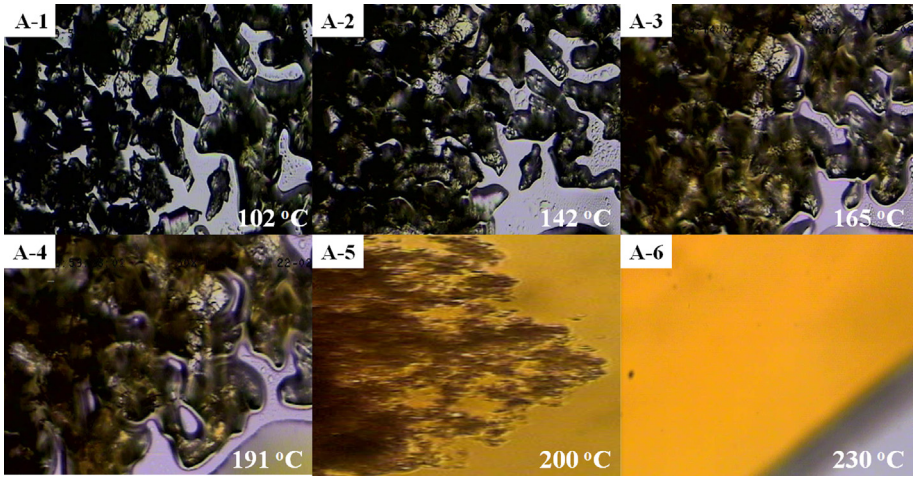

Fig. 8. Hot stage microscopy images of DIA-DHA eutectic showing the melting behaviour (A-1, before melting; A-2, 3, 4, starting to melt; A-5, melting at 200 ^{0}C and A-6, fully melted).

Table 4
Flow characteristic parameters of pure DIA, control batch and DIA-DHA eutectic.

Powder	Density (g/cc)		Carr's Index*	Hausner's ratio*	Flow Character#	Angle of repose*	Flow Character#
	Bulk	Tapped					
Pure DIA	0.3092	0.4562	32.22 ± 1.98	1.48 ± 0.08	Very poor	47.12 ± 1.21	Poor
Control batch	0.3158	0.4599	31.33 ± 1.34	1.46 ± 0.04	Very poor	44.73 ± 1.64	Passable
DIA-DHA eutectic	0.3846	0.4649	17.27 ± 0.8	1.21 ± 0.04	Fair	39.83 ± 1.28	Fair

* Indicates data shown as mean ± SD, (n = 3).
# As per US Pharmacopeia general chapter 1174.

Table 5
Comparison of packability, compatibility and compressibility study of pure DIA, control batch and DIA-DHA eutectic.

Parameters	Pure DIA	Control batch	DIA-DHA eutectic
a = 1/slope	0.585	0.513	0.432
1/b = intercept/slope	37.08	43.65	95.35
Kuno's constant, Kn	0.869	0.8851	1.812
Rearrangement index (ab index)	0.258	0.214	0.105
True density (g/cc)	1.062	1.2310	1.6040
Heckel plot constant, K	0.161	0.164	0.417
A	0.986	1.175	1.274
Yield pressure, Py	6.212	6.097	2.398
Yield strength, σ0	2.070	2.033	0.799
Tensile strength (kg/cm^2)*	4.59 ± 1.50	6.06 ± 2.17	12.59 ± 4.37
% Elastic recovery*	2.4778 ± 1.15	1.8527 ± 2.04	0.8706 ± 0.67

* Indicates data shown as mean ± SD, (n = 3).

diagram. The diagram showed a 'V'-shaped pattern which might be an indication for the formation of eutectic and not a cocrystal at the molar composition 25:75 [46,47].

3.1.2. PXRD study

The obtained diffractogram patterns of DIA, control batch, DHA, DIA-DHA eutectic and physical mixture are shown in Fig. 5. The powder XRD pattern of DIA revealed high intensity with characteristic sharp peaks at 2θ scattered angles of 10.5°, 17.4°, 21.9° and 27.9° which suggested the crystalline nature of drug [32]. In the case of DHA, characteristic intense peaks obtained at 13.5°, 26.8° and 28.4° (2θ) [33]. The characteristic diffraction peaks of pure drug, control batch crystal and coformer were still noticeable in the physical mixture as well as prepared sample also. It was further noticed that the intensity of diffraction peaks was much lower in the case of prepared sample compared to the diffraction peaks of pure components (Fig. 5). This might be due to reducing the drug's crystallinity [48]. This observation with almost no deviation in the diffraction peaks confirmed that the prepared sample was eutectic only [15].

3.1.3. ATR-FTIR analysis

IR spectra and the assignment of major bands of pure DIA, control batch, pure DHA, DIA-DHA physical mixture, and DIA-DHA eutectic sample are shown in Fig. 6 and Table SI2 (See in supplementary information). The IR spectrum of DIA revealed a broad O-H stretching band of –COOH group at wave number 3069 cm^{-1}, two carbonyl stretching strong bands at 1785 cm^{-1} (ester groups) and 1679 cm^{-1} (ketone group). The characteristic absorption spectra of DHA showed the wave number at 3490 cm^{-1}, 3560 cm^{-1} and 2900–3600 cm^{-1} (broad stretching vibration of carboxylic acid and hydroxyl group) and 1791 cm^{-1} (stretching vibration of carbonyl function group). It has been observed that FT-IR spectra of DIA-DHA eutectic described the summation of characteristic vibration bands corresponds to DIA and DHA molecules without any considerable shifting (Fig. 6(e)). Unchanged vibrational spectra exclude the formation of significant chemical interactions between drug and coformer. Moreover, a 'V'-shaped pattern in the binary phase diagram and no deviation in the diffraction peaks concluded the formation of eutectic rather the cocrystal [15,46].

3.1.4. SEM

The SEM study was executed to identify and compare the morphological characteristic among DIA, control batch, DHA and prepared eutectic as presented in Fig. 7. The SEM images of DIA (A-1

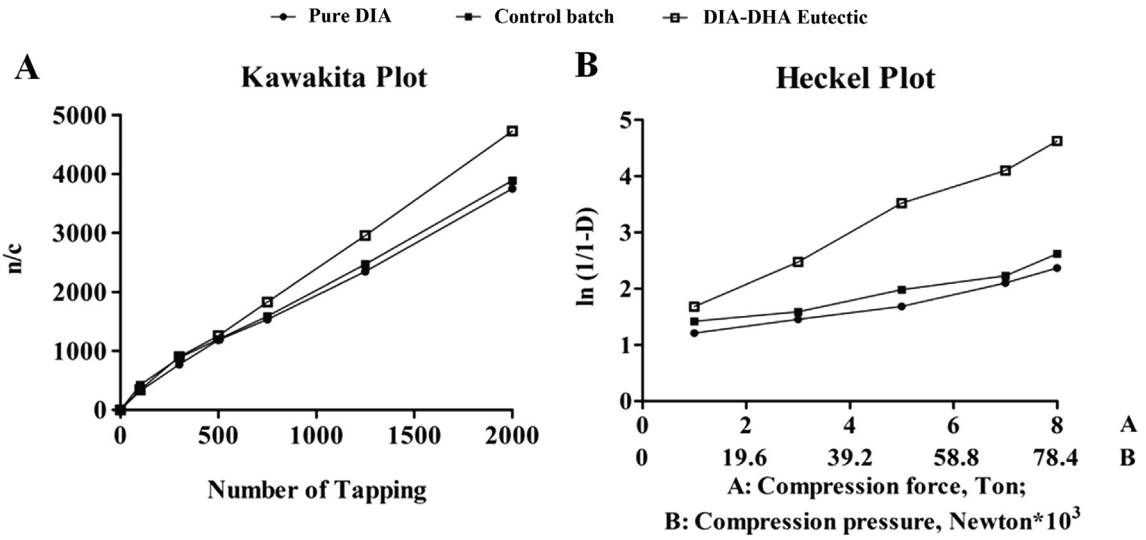

Fig. 9. (A) Kawakita plot and (B) Heckel plot of DIA; Control batch and DIA-DHA eutectic.

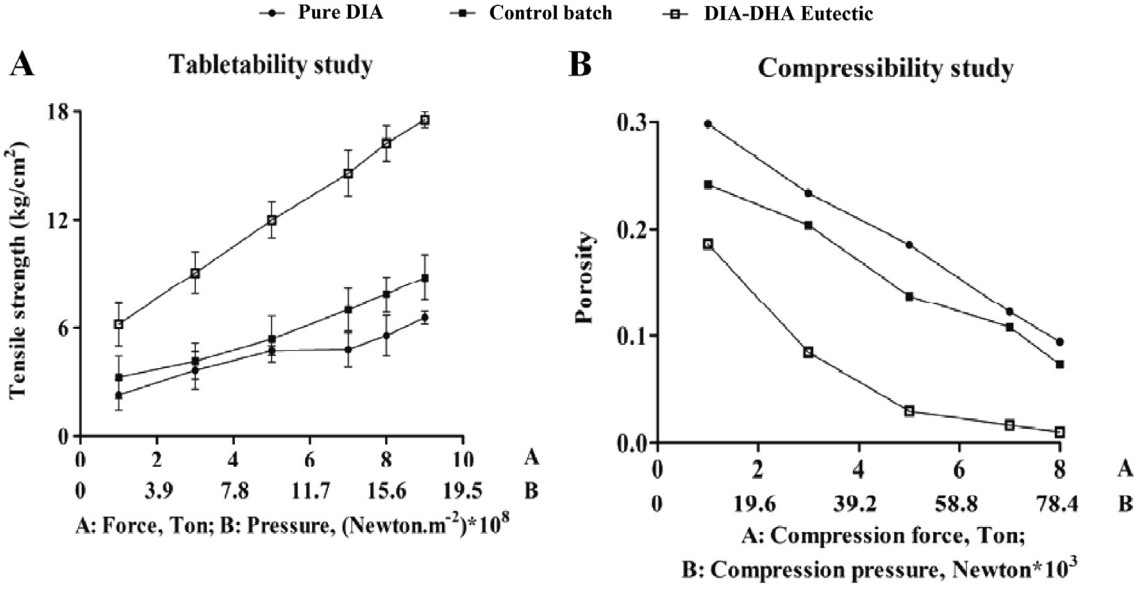

Fig. 10. (A) Tabletability and (B) Compressibility study of DIA; Control batch and DIA-DHA eutectic.

& A-2) and control batch (B-1 & B-2) were exhibited as acicular shaped crystalline particles which might be responsible for their poor flow properties. Crystals of eutectic sample (D-1 & D-2) showed platy shaped crystals with broadness in its shape along with shortening length compared to DIA and control batch crystals. It was further confirmed by measuring the aspect ratio (AR) of DIA crystals (AR = 4.9), control batch crystals (AR = 4.3) and eutectic crystals (AR = 1.2). This morphology of eutectic crystals imparted its role in the improvement of flow and compression property [49].

3.1.5. HSM study

The images from HSM study are shown in Fig. 8. Fig. 8(A-1) was an image of before melting of the eutectic sample. Various melting phases were observed by keeping the heating rate 10 °C/min from A-1 to A-2 as to achieve near to the melting point of the sample. From A-2 to A-6, the heating rate was reduced to 5 °C/min in order to observe the melting phases in a very careful manner. It was observed that the eutectic sample started melting at 190 °C and complete melting appeared at 230 °C which was purely in the coordination of DSC results of the eutectic sample [50].

3.2. Physicochemical and mechanical parameters

3.2.1. Flow characterization

The derived values of flow parameters obtained for pure drug, control batch and prepared eutectic are listed in Table 4. These results suggested that pure drug and control batch showed very poor flow characteristics with higher values of all measured parameters (Angle of repose, CI and Hausner's ratio), which could be attributed to the acicular shape and fluffy texture of pure drug and control batch resulted in high electrostatic charge [51]. Whereas, there was observed a noticeable improvement in flow characteristics of eutectic powder as compared to original drug. This could be ascribed to the reduction in aspect ratio of

the powder which imparted an equidimensional shape to the prepared eutectic sample [52].

3.2.2. Analysis of packability, compressibility, and compactibility

3.2.2.1. Packability study. Results of packability study could be expressed in terms of Kawakita and Kuno's constants. Values of Kawakita constants '*a*' and '*1/b*' for pure drug, control batch and prepared sample are listed in Table 5 and the plot is represented in Fig. 9(A). In this investigation, a linear relationship was observed throughout the whole range of tapping with a correlation coefficient of more than 0.99. Kawakita equation explained that the decreased values of '*a*' (total compressibility of material or extent of densification due to tapping) and increased values of '*1/b*' (cohesive property of powder or how fast/easily the final packing state was achieved) compared with the values of the pure drug and control batch was an indication of the improvement in packability of the prepared sample. Prepared eutectic showed increased values of *Kn* (Kuno's constant), which imparted a greater packability as compared with DIA and control batch [53]. The value of ab index in case of the eutectic sample was lower compared to pure drug and control batch which was an indication for the requirement of less number of tapping for the particle rearrangement for the eutectic sample [36].

3.2.2.2. Heckel study. The pure drug by appearance was fluffy powder and also revealed by a lower true density when compared to the prepared sample as listed in Table 5. The Heckel plot parameters in which increased value of 'K' of prepared sample as compared to pure drug and control batch have greater plastic behaviour of the powder. Furthermore, a higher value of 'A' over the pure drug which led to the increased propensity of material fragmentation and particle rearrangement. This fragmentation of larger particles produces small particles which played a significant role in void filling resulting in increased relative density in the prepared sample. The yield strength ($\sigma 0$) and yield pressure (Py) values were calculated from the linear portion of the Heckel plot

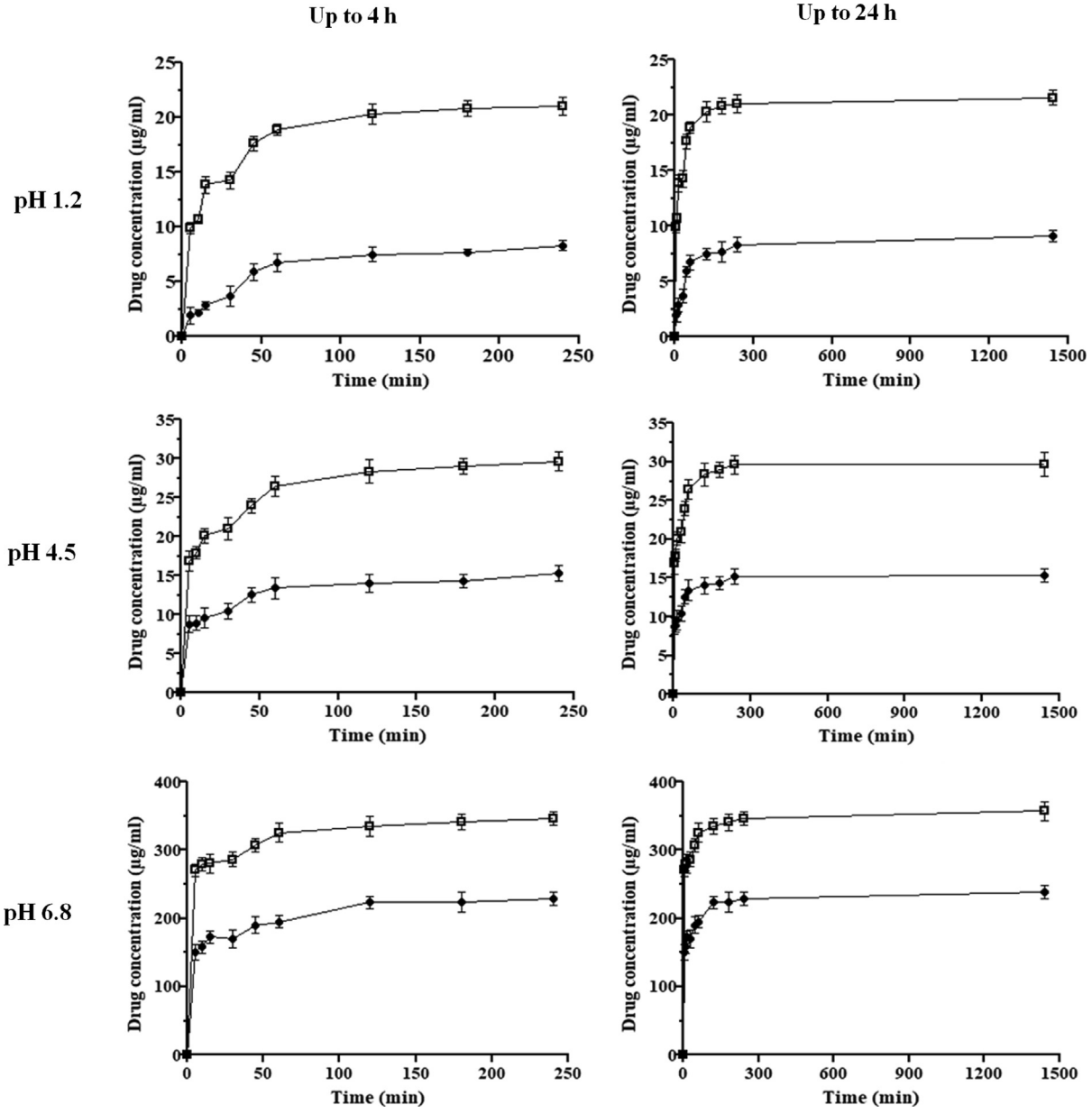

Fig. 11. Kinetic solubility measurements of DIA and DIA-DHA eutectic at pH 1.2, pH 4.5 and pH 6.8 during the first 4 h and throughout 24 h of the experiment.

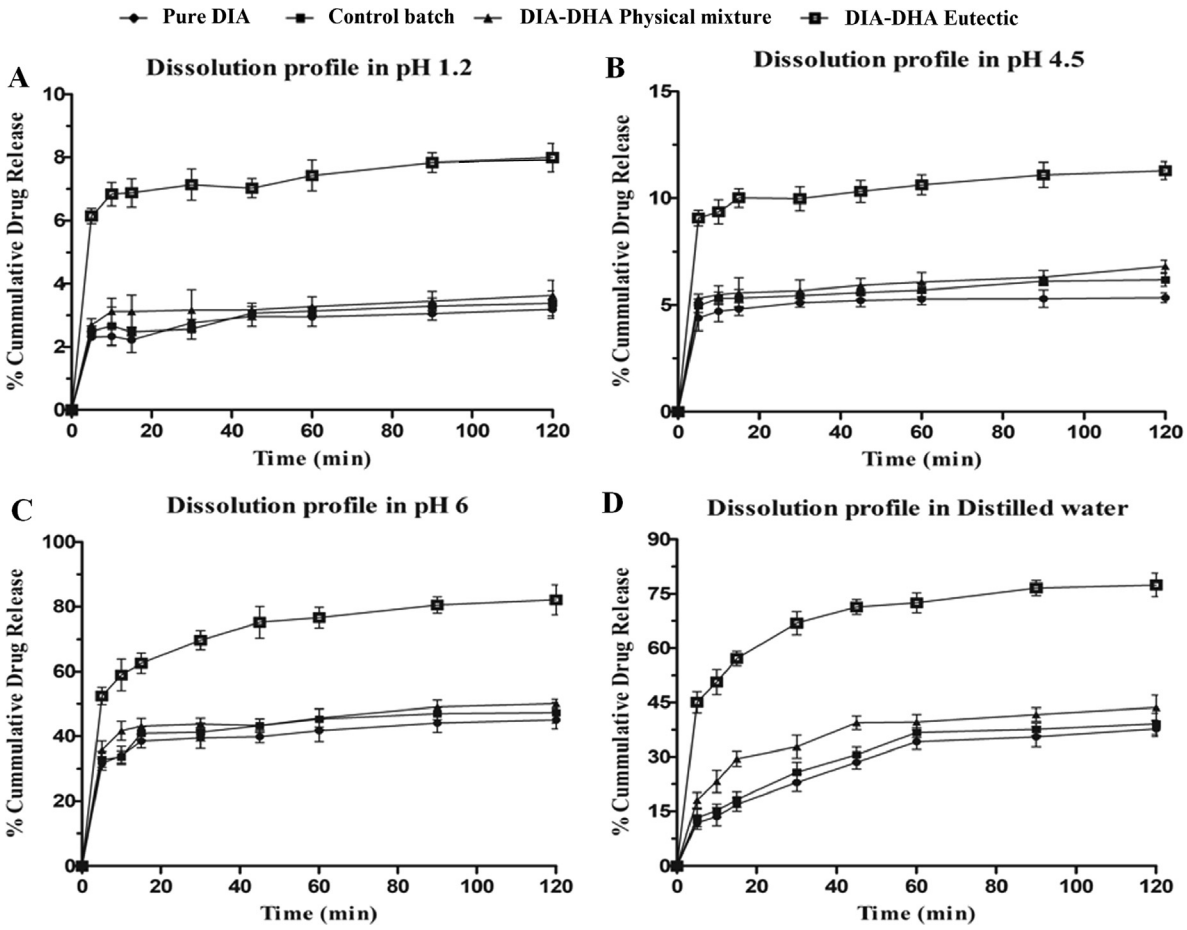

Fig. 12. *In-vitro* drug release profile of powder formulation in (A) pH 1.2; (B) pH 4.5; (C) pH 6 and (D) Distilled water.

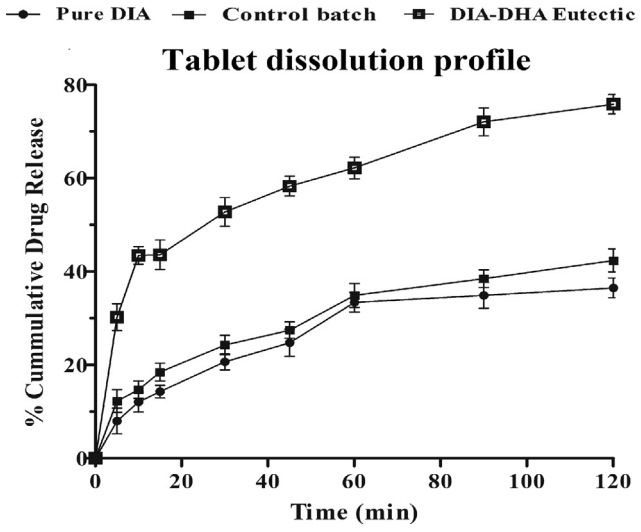

Fig. 13. *In-vitro* drug release profile of tablet formulation of DIA; Control batch and DIA-DHA eutectic in pH 6.

(R^2 > 0.98 in all prepared samples). Heckel analysis depicted the lower Py and σ0 values for the prepared sample as compared to pure drug was a sign of better compression property as shown in Fig. 9 (B). Another observation was made from the Heckel plot that the initial curvature in the graph was absent. It was an indication of the fragmentation behaviour of the material. Pure drug shows fragmentation behaviour with very low brittleness index. Due to which lamination was resulting with even at very low pressure during Heckel analysis, a small amount of 2% w/w MCC was added with pure drug, control batch and eutectic sample followed by the Heckel study at various ascending pressures. From the slope 'A' of all the Heckel curves, it was observed that the fragmentation and formation of new surfaces were greater in the eutectic sample compared to pure drug and control batch. The above result reveals that the prepared material has become more suitable as compared to the pure drug and control batch as far as the tablet manufacturing is concerned using direct compression technique [54].

3.2.2.3. Tensile strength and elastic recovery measurement. Tensile strength of all powders increased with compression pressure Fig. 10 (A). However, the prepared sample showed higher tensile strength over pure drug at all compression pressures. Thus, the powder of prepared sample is more suitable for tabletability as compared to pure drug and control batch [55]. As shown in Fig. 10(B), the porosity of material was reduced with an increase in the compression pressure. Moreover, this tendency was intensified in the case of eutectic sample which was an indication of improved compressibility behaviour of eutectic sample [39]. By comparing the elastic recovery of drug, control batch and prepared sample, it was clear that the prepared sample is more plastic in nature than the parent drug (Table 5). These results can be well correlated with the studies by Rowe and Roberts (1987) [56].

3.2.3. Evaluation of directly compressible tablets

Tablet formulation of pure DIA and control batch formulas required 10% w/w of MCC compared to the eutectic formula where

Table 6
Values $\%DP_{10\ min}$, $\%\ DE_{10\ min}$, MDT, f_1 and f_2 for powder and formulation in different dissolution media.

Parameters		Distilled water	pH 1.2	pH 4.5	pH 6	
		P	**P**	**P**	**P**	**T**
Pure DIA	$\%DP_{10\ min}$	13.55	2.34	4.71	33.05	29.71
	$\%\ DE_{10\ min}$	1.55	1.09	1.26	8.05	6.19
	MDT	–	–	–	21.70	23.84
	f_1, f_2	–	–	–	–	–
Control batch	$\%DP_{10\ min}$	15.18	2.66	5.42	34.54	32.62
	$\%\ DE_{10\ min}$	1.73	1.31	1.78	8.83	7.04
	MDT	–	–	–	20.93	22.11
	f_1, f_2	–	–	–	8.47, 69.55	15,35, 70.56
Physical mixture	$\%DP_{10\ min}$	18.09	3.12	5.58	39.69	–
	$\%\ DE_{10\ min}$	2.16	1.39	2.54	9.10	–
	MDT	–	–	–	–	–
	f_1, f_2	–	–	–	–	–
Prepared eutectic	$\%DP_{10\ min}$	25.34	6.83	9.36	58.91	53.46
	$\%\ DE_{10\ min}$	5.87	3.80	4.91	11.82	10.33
	MDT	–	–	–	12.19	13.05
	f_1, f_2	–	–	–	77,50, 25.39	83.30, 24.65

*Buffer: Hydrochloric acid buffer (pH 1.2); Acetate buffer (pH 4.5); Citrate buffer (pH 6).
$MDT_{in\ vitro}$, f_1 and f_2 values of powder and tablet formulation of pure DIA, control batch and prepared eutectic have evaluated in citrate buffer (pH 6).
Tablet dissolutions of pure DIA, control batch and prepared eutectic were only evaluated in official media (pH 6).
P – Indicates powder dissolution; T – Indicates tablet dissolution.

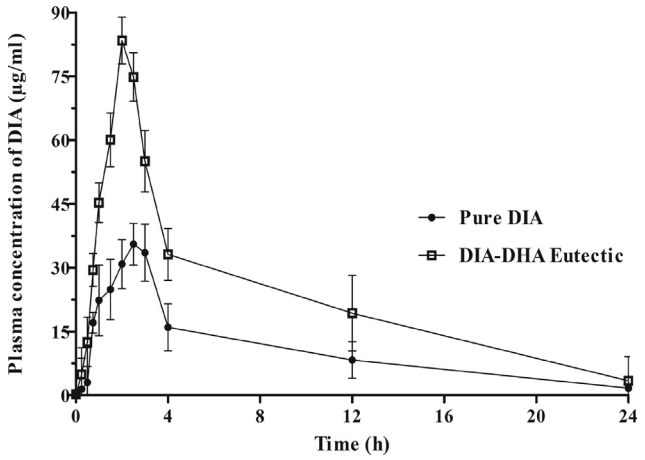

Fig. 14. Mean plasma concentration-time curves of DIA and DIA-DHA eutectic.

Table 7
Pharmacokinetic parameters of DIA and prepared eutectic after single oral dose administration to Sprague-Dawley rats.

Parameters*	DIA	DIA-DHA eutectic
C_{max} (µg/ml)	35.54 ± 5.72	83.43 ± 4.57
T_{max} (h)	2.5 ± 0.92	2 ± 0.66
$AUC_{0\text{-}24h}$ (µg h/ml)	249.91 ± 152.43	542.02 ± 202.93
AUC_{total} (µg h/ml)	298.60 ± 141.19	621.27 ± 389.41
$T_{1/2}$ (h)	9.8 ± 2.39	8.02 ± 1.87
VD (l)	21.22 ± 4.01	15.10 ± 2.94
CL (l/h)	0.74 ± 0.26	0.65 ± 0.19
AUMC (µg h^2/ml)	1174.28 ± 308.50	2348.56 ± 653.13
MRT (h)	3.93 ± 1.53	4.68 ± 2.04
F_{rel}	1	2.08

* Indicates data shown as mean ± SD, (n = 6).

only 2% w/w of MCC was required. It indicated that the eutectic sample could be compressed more easily in the form of tablet compared to pure drug and control batch. The manufacturing formulas and evaluation parameters of directly compressible tablets of all materials are shown in Table 1. All evaluation parameters were shown in good accordance with acceptance criteria [57].

3.2.4. HPLC method development

DIA showed pH-dependent solubility due to the weakly acidic nature, which enhances solubility at higher pH and reduces solubility at lower pH. Furthermore, it has been seen that the buffer solutions at pH $\geq$ 5 represented the quantification of DIA in the form of rhein as all DIA converted to its active metabolite rhein form [27]. A simple HPLC method was developed and validated for the estimation of DIA and rhein in the prepared samples as per ICH guideline Q2(R1) [58]. The detailed HPLC parameters of DIA, DHA and rhein were tabulated in Table SI3, see supplementary information. The HPLC chromatogram depicted the retention time (Rt) for the standard solution of DIA, DHA and rhein to be 10.5, 6.6, and 11.6 min, respectively (Fig. SI1, see supplementary information).

3.2.5. % yield and drug content

% Yield and drug content of DIA-DHA eutectic were found to be 94.55 ± 0.81 and 85.89 ± 2.43 respectively which showed satisfactory results. The drug content of the prepared eutectic indicated good recovery of the drug after eutectic formation.

3.2.6. Kinetic solubility measurements

Kinetic solubility of DIA and DIA-DHA eutectic in different buffer solutions were explored and quantification of the drug was done by HPLC as depicted graphically in Fig. 11. The kinetic solubility profiles of DIA in pH 1.2, pH 4.5, and pH 6.8 at 4 h exhibited 8.33, 15.27, and 229.13 µg/ml respectively and subsequently reached a plateau (Fig. 11). These values indicated that DIA showed pH-dependent solubility. For the data of DIA-DHA eutectic, the solubility in pH 6.8 at 4 h achieved maximum values 345.76 µg/ml while the solubility measurements in pH 1.2 and pH 4.5 were found to be 21.02 and 29.63 µg/ml respectively at 4 h. At the different buffer solutions, the prepared eutectic revealed the improvement in solubility with 2.5, 1.9 and 1.5 folds at pH 1.2, pH 4.5 and pH 6.8, respectively as compared to pure DIA. From 4 to 24 h, the concentration of DIA in pH 1.2, pH 4.5, and pH 6.8 solutions increased a mere 8.5%, 9.9% and 9.6% and reached an apparent solubility of 9.10, 15.33 and 238.86 µg/ml, respectively. For the prepared eutectic, the apparent solubility in pH 1.2, pH 4.5, and pH 6.8 solutions were enhanced 2.4, 1.9, and 1.5 times respectively, compared to the pure DIA. Additionally, the apparent solubility was also estimated in pH 6 solution and was found to be

2.0 times higher than the pure drug (Data not shown). The results of solubility measurement were shown that all the prepared eutectic also exhibited pH-dependent solubility. It has been reported that multi-component adduct comprised of poorly soluble API with more soluble coformer will be ascribed by solubilization of coformer in the solution which might exhibit the enhancement of solubility. During the solubility experiment, DHA molecules diffused in the buffer solution faster than the parent DIA because the molecular weight is smaller than that of DIA as well as DHA exhibits a strong affinity towards the water molecules. Consequently, the less soluble DIA molecules become supersaturated in the solution as an amorphous phase which may result in the improvement in the kinetic solubility of prepared eutectic as compared to pure DIA [59].

3.2.7. In-vitro drug release profile

As shown in Figs. 12 and 13, the powder and tablet dissolution of DIA-DHA eutectic was improved a greater extent compared to pure DIA, control batch and physical mixture samples. The statistical parameters for the comparison of dissolution profile of all the samples in various dissolution media are summarized in Table 6. The possible mechanism behind the enhancement in dissolution rate of powder and tablet prepared from eutectic was attributed to the release of ultrafine crystals into the dissolution media. Furthermore, the excess of coformer in the solution modulates thermodynamic stability (i.e. dissociation) in context to crystal packing, molecular mobility and intermolecular interaction [60,61]. Restricted solubility of DIA in the lower pH range, which ultimately leads to poor bioavailability, at the same time prepared eutectic showed an enhancement in dissolution in all pH ranges.

3.3. Pharmacokinetic study

The average plasma concentration-time curves of pure drug and prepared eutectic after single oral dose administration were estimated in SD rats as shown in Fig. 14 and the pharmacokinetic parameters are summarized in Table 7. The maximum plasma concentration (C_{max}) achieved was nearer 2.3 times higher for prepared eutectic and also the time to reach maximum plasma concentration was decreased from 2.5 h to 2 h as compared to parent DIA. This result suggests the improved rate of absorption with the administration of prepared eutectic. It is manifested that each time point the plasma concentration of prepared eutectic was remarkably higher than those administrated with the pure DIA. Relative bioavailability (F_{rel}) was calculated as the ratio of AUC_{total} (eutectic) to AUC_{total} (DIA). This finding suggested that prepared eutectic exhibited 2.08 folds more orally bioavailable than the pure DIA. An enhancement in the pharmacokinetic parameters of the novel eutectic form of DIA was the indication for improvement in the oral bioavailability of pure drug [62].

3.4. Stability study

The dissolution profiles of prepared eutectic (both powder and tablet) were evaluated in pH 6 and found to be similar before and after study. The statistical data were also attested similarity between two dissolution profiles which were found f_2 = 70.32 for powder and f_2 = 76.86 for tablet formulation before and after study (Graph not shown here). Moreover, the physical changes of samples were investigated using DSC and PXRD analysis. The characteristic peaks of the eutectic samples in the PXRD pattern and IR spectra were still evident as well as DSC thermograms remained unchanged as compared to the initial samples (Data shown in supplementary Figs. SI2, SI3 and SI4). Hence, the prepared eutectic sample bestows stability advantages and found to be stable in nature.

4. Conclusion

The present investigation was done to explore the way how to detect and interpret the multi-component system using binary phase diagram by taking DIA as BCS class II drug. A eutectic mixture of DIA with DHA in the molar composition of 1:3 was formulated using acetone assistant grinding technique. The resulting eutectic proved significant improvement in its physicochemical as well as mechanical properties compared to pure drug and control batch. The equidimensional shape of the particles with its platy nature imparted good flow and compressibility to the eutectic solid form. The drug and coformer have interacted with each other (intermolecular) which was not possible in case of the physical mixture. This could change the entire functionality of the pure drug. Bioavailability was greatly enhanced in case of the eutectic solid form along with its stable nature. The present study concluded that the multi-component system can become a potential way to simultaneously improve physicochemical and mechanical properties of poorly water-soluble and compressible APIs and can be used commercially for the development of directly compressible solid orals.

Acknowledgements

The author gratefully acknowledges Department of Science and Technology (DST), New Delhi, India, for providing DST-INSPIRE Fellowship to carry out this research work. Authors are grateful to Prof. Arvind Bansal, Head, Department of Pharmaceutics, NIPER-Mohali, Prof. Changquan Calvin Sun, Professor, Department of Pharmaceutics, University of Minnesota, USA and Mr. Dnyaneshwar Kale, PhD student, Department of Pharmaceutics, NIPER-Mohali, for their continuous guidance and support throughout the study.

Appendix A. Supplementary data

Supplementary data to this article can be found online at https://doi.org/10.1016/j.apt.2020.01.021.

References

[1] S. Stegemann, F. Leveiller, D. Franchi, H. De Jong, H. Lindén, When poor solubility becomes an issue: from early stage to proof of concept, Eur. J. Pharm. Sci. 31 (2007) 249–1246.
[2] C.C. Sun, Cocrystallization for successful drug delivery, Expert Opin. Drug Deliv. 10 (2013) 201–213.
[3] C.R. Gardner, C.T. Walsh, Ö. Almarsson, Drugs as materials: valuing physical form in drug discovery, Nat. Rev. Drug Discov. 3 (2004) 926–934.
[4] G.R. Desiraju, Supramolecular synthons in crystal engineering—a new organic synthesis, Angew Chem. Int. Ed. Engl. 34 (1995) 2311–2327.
[5] N.K. Duggirala, M.L. Perry, Ö. Almarsson, M.J. Zaworotko, Pharmaceutical cocrystals: along the path to improved medicines, Chem. Commun. 52 (2016) 640–655.
[6] Z. Rahman, A. Siddiqui, M.A. Khan, Orally disintegrating tablet of novel salt of antiepileptic drug: formulation strategy and evaluation, Eur. J. Pharm. Biopharm. 85 (2013) 1300–1309.
[7] R.W. Lancaster, P.G. Karamertzanis, A.T. Hulme, D.A. Tocher, T.C. Lewis, S.L. Price, The polymorphism of progesterone: stabilization of a 'disappearing' polymorph by co-crystallization, J. Pharm. Sci. 96 (2007) 3419–3431.
[8] E.C. Van Tonder, M.D. Mahlatji, S.F. Malan, W. Liebenberg, M.R. Caira, M. Song, M.M. De Villiers, Preparation and physicochemical characterization of 5 niclosamide solvates and 1 hemisolvate, AAPS PharmSciTech. 5 (2004) 86.
[9] D. Giron, C. Goldbronn, M. Mutz, S. Pfeffer, P. Piechon, P. Schwab, Solid state characterizations of pharmaceutical hydrates, J. Therm. Anal. Calorim. 68 (2002) 453–465.
[10] S. Ren, M. Liu, C. Hong, G. Li, J. Sun, J. Wang, L. Zhang, Y. Xie, The effects of pH, surfactant, ion concentration, coformer, and molecular arrangement on the solubility behavior of myricetin cocrystals, Acta Pharm. Sin. B. 9 (2019) 59–73.
[11] R.D. Patel, M.K. Raval, A.A. Bagathariya, N.R. Sheth, Functionality improvement of Nimesulide by eutectic formation with nicotinamide: exploration using temperature-composition phase diagram, Adv. Powder. Technol. 30 (2019) 961–973.

[12] S. Chakraborty, G.R. Desiraju, C-H··· F hydrogen bonds in solid solutions of benzoic acid and 4-fluorobenzoic acid, Cryst. Growth Des. 18 (2018) 3607–3615.
[13] K. Suresh, M.C. Mannava, A. Nangia, A novel curcumin–artemisinin coamorphous solid: physical properties and pharmacokinetic profile, RSC Adv. 4 (2014) 58357–58361.
[14] G.R. Desiraju, Crystal engineering: from molecule to crystal, J. Am. Chem. Soc. 135 (2013) 9952–9967.
[15] S. Cherukuvada, A. Nangia, Eutectics as improved pharmaceutical materials: design, properties and characterization, Chem. Commun. 50 (2014) 906–923.
[16] S. Cherukuvada, T.N. Guru Row, Comprehending the formation of eutectics and cocrystals in terms of design and their structural interrelationships, Cryst. Growth Des. 14 (2014) 4187–4198.
[17] S.G. Khare, S.K. Jena, A.T. Sangamwar, S. Khullar, S.K. Mandal, Multicomponent pharmaceutical adducts of α-eprosartan: physicochemical properties and pharmacokinetic study, Cryst. Growth Des. 17 (2017) 1589–1599.
[18] K. Chadha, M. Karan, R. Chadha, Y. Bhalla, K. Vasisht, Is failure of cocrystallization actually a failure? Eutectic formation in cocrystal screening of hesperetin, J. Pharm. Sci. 106 (2017) 2026–2036.
[19] I. Sathisaran, S.V. Dalvi, Crystal engineering of curcumin with salicylic acid and hydroxyquinol as conformers, Cryst. Growth Des. 17 (2017) 3974–3988.
[20] H. Jain, K.S. Khomane, A.K. Bansal, Implication of microstructure on the mechanical behaviour of an aspirin–paracetamol eutectic mixture, Cryst. Eng. Comm. 16 (2014) 8471–8478.
[21] R. Chadha, M. Sharma, J. Haneef, Multicomponent solid forms of felodipine: preparation, characterisation, physicochemical and in-vivo studies, J. Pharm. Pharmacol. 69 (2017) 254–264.
[22] R. Thipparaboina, D. Thumuri, R. Chavan, V.G. Naidu, N.R. Shastri, Fast dissolving drug-drug eutectics with improved compressibility and synergistic effects, Eur. J. Pharm. Sci. 104 (2017) 82–89.
[23] J. Haneef, R. Chadha, Drug-drug multicomponent solid forms: cocrystal, coamorphous and eutectic of three poorly soluble antihypertensive drugs using mechanochemical approach, AAPS PharmSciTech. 18 (2017) 2279–2290.
[24] A. Górniak, B. Karolewicz, E. Żurawska-Płaksej, J. Pluta, Thermal, spectroscopic, and dissolution studies of the simvastatin–acetylsalicylic acid mixtures, J. Therm. Anal. Calorim. 111 (2013) 2125–2132.
[25] P. Nicolas, M. Tod, C. Padoin, O. Petitjean, Clinical pharmacokinetics of diacerein, Clin. Pharmacokinet. 35 (1998) 347–359.
[26] I. Elsayed, A.A. Abdelbary, A.H. Elshafeey, Nanosizing of a poorly soluble drug: technique optimization, factorial analysis, and pharmacokinetic study in healthy human volunteers, Int. J. Nanomedicine. 9 (2014) 2943–2953.
[27] D.K. Batt, K.C. Garala, Preparation and evaluation of inclusion complexes of diacerein with β-cyclodextrin and hydroxypropyl β-cyclodextrin, J. Incl. Phenom. Macrocycl. Chem. 77 (2013) 471–481.
[28] H.M. El-Laithy, E.B. Basalious, B.M. El-Hoseiny, M.M. Adel, Novel self-nanoemulsifying self-nanosuspension (SNESNS) for enhancing oral bioavailability of diacerein: simultaneous portal blood absorption and lymphatic delivery, Int. J. Pharm. 490 (2015) 146–154.
[29] A.K. Aggarwal, S. Singh, Physicochemical characterization and dissolution study of solid dispersions of diacerein with polyethylene glycol 6000, Drug Dev. Ind. Pharm. 37 (2011) 1181–1191.
[30] M.I. Khan, A. Madni, L. Peltonen, Development and in-vitro characterization of sorbitan monolaurate and poloxamer 184 based niosomes for oral delivery of diacerein, Eur. J. Pharm. Sci. 95 (2016) 88–95.
[31] R. Malik, T. Garg, A.K. Goyal, G. Rath, Diacerein-Loaded novel gastroretentive nanofiber system using PLLA: development and in vitro characterization, Artif. Cells Nanomed. Biotechnol. 44 (2016) 928–936.
[32] A. Jain, S.K. Singh, Y. Singh, S. Singh, Development of lipid nanoparticles of diacerein, an antiosteoarthritic drug for enhancement in bioavailability and reduction in its side effects, J. Biomed. Nanotechnol. 9 (2013) 891–900.
[33] R. Kaur, R. Gautam, S. Cherukuvada, T.N. Guru Row, Do carboximide–carboxylic acid combinations form co-crystals? The role of hydroxyl substitution on the formation of co-crystals and eutectics, IUCrJ. 2 (2015) 341–351.
[34] M.K. Raval, P.D. Vaghela, A.N. Vachhani, N.R. Sheth, Role of excipients in the crystallization of albendazole, Adv. Powder Technol. 26 (2015) 1102–1115.
[35] P.J. Denny, Compaction equations: a comparison of the Heckel and Kawakita equations, Powder Technol. 127 (2002) 162–172.
[36] J. Nordström, I. Klevan, G. Alderborn, A particle rearrangement index based on the Kawakita powder compression equation, J. Pharm. Sci. 98 (2009) 1053–1063.
[37] S. Patel, A.M. Kaushal, A.K. Bansal, Compaction behavior of roller compacted ibuprofen, Eur. J. Pharm. Biopharm. 69 (2008) 743–749.
[38] B.S. Barot, P.B. Parejiya, T.M. Patel, R.K. Parikh, M.C. Gohel, Compactibility improvement of metformin hydrochloride by crystallization technique, Adv. Powder Technol. 23 (2012) 814–823.
[39] J.T. Fell, J.M. Newton, Determination of tablet strength by the diametral-compression test, J. Pharm. Sci. 59 (1970) 688–691.
[40] N.A. Armstrong, R.F. Haines-Nutt, Elastic recovery and surface area changes in compacted powder systems, Powder Technol. 9 (1974) 287–290.
[41] Anonymous, Indian Pharmacopoeia. Vol. III, Government of India Ministry of Health & Family Welfare, The Controller of Publications, New Delhi, India, 2010, pp. 1191–1193.
[42] N.H. Anderson, M. Bauer, N. Boussac, R. Khan-Malek, P. Munden, M. Sardaro, An evaluation of fit factors and dissolution efficiency for the comparison of in vitro dissolution profiles, J. Pharm. Biomed. Anal. 17 (1998) 811–822.
[43] A.J. Cruz-Cabeza, Acid–base crystalline complexes and the pK a rule, Cryst. Eng. Comm. 14 (2012) 6362–6365.
[44] T. Friscic, W. Jones, Recent advances in understanding the mechanism of cocrystal formation via grinding, Cryst. Growth Des. 9 (2009) 1621–1637.
[45] W.J. Irwin, M. Iqbal, Solid-state stability: the effect of grinding solvated excipients, Int. J. Pharm. 75 (1991) 211–218.
[46] E.V. Agafonova, Y.V. Moshchenskiy, M.L. Tkachenko, DSC study and calculation of metronidazole and clarithromycin thermodynamic melting parameters for individual substances and for eutectic mixture, Thermochim. Acta 580 (2014) 1–6.
[47] S.G. Avula, K. Alexander, A. Riga, Thermal analytical characterization of mixtures of antipsychotic drugs with various excipients for improved drug delivery, J. Therm. Anal. Calorim. 123 (2016) 1981–1992.
[48] M.K. Raval, K.R. Sorathiya, N.P. Chauhan, J.M. Patel, R.K. Parikh, N.R. Sheth, Influence of polymers/excipients on development of agglomerated crystals of secnidazole by crystallo-co-agglomeration technique to improve processability, Drug Dev. Ind. Pharm. 39 (2013) 437–446.
[49] P.P. Shah, R.C. Mashru, Development and evaluation of artemether taste masked rapid disintegrating tablets with improved dissolution using solid dispersion technique, AAPS PharmSciTech. 9 (2008) 494–500.
[50] I.M. Vitez, A.W. Newman, M. Davidovich, C. Kiesnowski, The evolution of hot-stage microscopy to aid solid-state characterizations of pharmaceutical solids, Thermochim. Acta 324 (1998) 187–196.
[51] A.K. Tiwary, G.M. Panpalia, Influence of crystal habit on trimethoprim suspension formulation, Pharm. Res. 16 (1999) 261–265.
[52] Y. Kawashima, M. Imai, H. Takeuchi, H. Yamamoto, K. Kamiya, T. Hino, Improved flowability and compactibility of spherically agglomerated crystals of ascorbic acid for direct tableting designed by spherical crystallization process, Powder Technol. 130 (2003) 283–289.
[53] A. Hassanpour, M. Ghadiri, Distinct element analysis and experimental evaluation of the Heckel analysis of bulk powder compression, Powder Technol. 141 (2004) 251–261.
[54] Y. Kawashima, F. Cui, H. Takeuchi, T. Niwa, T. Hino, K. Kiuchi, Improvement in flowability and compressibility of pharmaceutical crystals for direct tabletting by spherical crystallization with a two solvent system, Powder Technol. 78 (1994) 151–156.
[55] C.C. Sun, Decoding powder tabletability: roles of particle adhesion and plasticity, J. Adhes. Sci. Technol. 25 (2011) 483–499.
[56] R.J. Roberts, R.C. Rowe, The compaction of pharmaceutical and other model materials – a pragmatic approach, Chem. Eng. Sci. 42 (1987) 903–911.
[57] G. Abdelbary, C. Eouani, P. Prinderre, J. Joachim, J.P. Reynier, P.H. Piccerelle, Determination of the in vitro disintegration profile of rapidly disintegrating tablets and correlation with oral disintegration, Int. J. Pharm. 292 (2005) 29–41.
[58] ICH Harmonized Tripartite Guideline, Validation of analytical procedures: Text and Methodology Q2 (R1), International Conference on Harmonization. Geneva, Switzerland, November 2005. http://www.ich.org/fileadmin/Public_web_Site/ICH_Products/Guidelines/Quality/Q2_R1/Step4/Q2_R1_Guideline.pdf (accessed on August 31st, 2019).
[59] D.J. Good, N. Rodríguez-Hornedo, Cocrystal eutectic constants and prediction of solubility behavior, Cryst. Growth Des. 10 (2010) 1028–1032.
[60] S. Cherukuvada, On the issues of resolving a low melting combination as a definite eutectic or an elusive cocrystal: a critical evaluation, J. Chem. Sci. 128 (2016) 487–499.
[61] N.R. Goud, K. Suresh, P. Sanphui, A. Nangia, Fast dissolving eutectic compositions of curcumin, Int. J. Pharm. 439 (2012) 63–72.
[62] A.H. Goldberg, M. Gibaldi, J.L. Kanig, Increasing dissolution rates and gastrointestinal absorption of drugs via solid solutions and eutectic mixtures III: Experimental evaluation of griseofulvin-succinic acid solid solution, J. Pharm. Sci. 55 (1966) 487–492.